### 1.3.3 Subwavelength light control with semiconductor nanowires

*Semiconductor nanostructures with large dielectric constant and high aspect ratio such as nanowires (NWs) represent a formidable playground for the study of the light-matter interaction as well as for nanophotonic, nano-optic and nanoplasmonic applications. The manipulation of light below the diffraction limit enabled by the use of semiconductor NWs attracts much attention owing to its potential impact on sensing and microscopy, as well as on computation and communication technologies. Here we report in brief our recent achievements in demonstrating semiconductor nanowire–based systems and devices for subwavelength light emission, scattering, guiding and reflection.*

Building on our expertise in the InAs/InP NW growth technology we engineered InP-InAs-InP multi-shell NWs that behave as polychromatic emitters in the energy range from 0.7 to 1.6 eV [1]. The photoluminescence (PL) emission from these individual nanostructures displays different features ascribable to distinct emitting domains, including InAs quantum dot and quantum well, as well as crystal-phase quantum disks arising from the coexistence of InP zincblende (ZB) and wurtzite (WZ) segments in the same NW. These crystal-phase low-dimensional structures offer great potential for the implementation of photonic devices of interest for quantum information processing. In this context, we reported on the anisotropy of the g-factor tensor and diamagnetic coefficient in WZ/ZB crystal-phase quantum dots (QDs) realized in single InP nanowires (Fig. 1) [2]: the electron (hole) g-factor tensor and the exciton diamagnetic coefficients were determined through micro-PL measurements at 4.2 K with different magnetic field configurations, and rationalized by invoking the spin-correlated orbital current model. Overall, our single NW emitters can find applications as optically active components in nanodevices for quantum information and communication technologies.

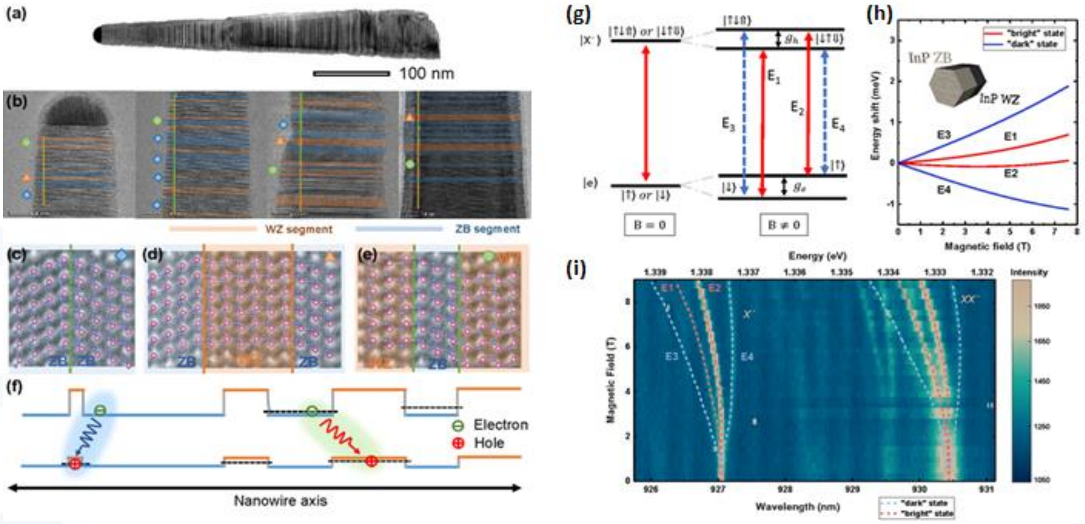

**Figure 1. (a)** Dark field STEM image of a mixed WZ/ZB InP NW. **(b)** STEM-HAADF images of different InP NW segments. Different symbols correspond to different structures depicted in Fig. **(c)-(e)**, where the ball-and-stick model of different segments and atomic resolution STEM images are reported. **(f)** Schematic energy level of the WZ/ZB sequence in the InP NW. **(g)** Energy diagram of the negatively-charged-exciton with $B$ perpendicular to the growth axis. **(h)** Energy shift of the four possible transitions of charged exciton, as a function of $B$. **(i)** Magneto-PL spectra of $X^-$ and $XX^-$ with $B_{\text{out-of-plane}}$ from 0 to 9 T.

Besides, we engineered individual semiconductor nanowire devices that allowed us to demonstrate a novel technique for the realization of subwavelength light sources operating at 1 GHz [3]. Light sources with nanoscale emission spots are regarded as an alternative tool to aperture-based near-field optical systems for the implementation of microscopy techniques not subjected to the diffraction limit. We realized hybrid metal-GaAs nanowire devices by controlled thermal annealing of Ni/Au electrodes, and investigated the metallic phases observed in the nanostructure body. Devices were fabricated onto a SiN membrane compatible with transmission electron microscopy studies. Energy dispersive X-ray spectroscopy allowed us to show that the nanowire body includes two Ni-rich phases, that thanks to an innovative use of electron diffraction tomography were unambiguously identified as Ni3GaAs and Ni5As2 crystals [4]. Using the annealing technique, we prepared hybrid metal–GaAs nanowires embedding two sharp axial Schottky barriers acting as nanoscale point-sources of light. Visible-light electroluminescence was reported upon suitable voltage biasing of the junctions. We investigated the time-resolved emission properties of our devices and demonstrated an electrical modulation of light generation up to 1 GHz. We explored different drive configurations and discussed the intrinsic bottlenecks of the presented device architecture. Our results demonstrated a novel technique for the realization of fast subwavelength light sources, with possible applications in sensing and microscopy beyond the diffraction limit.

Another research activity focused on mesoscale and nanoscale systems with a topology characterized by bends or crossings - such as *V*-, *T*- or *Y*-shaped, crosswise or multi-armed structures – that provide a fascinating playground for the study of guiding and interference phenomena. We focused on individual multibranched $SnO_2$ nanostructures with “nodes” i.e. locations where two or more branches originate, and we studied how light propagates when a laser source is focused onto a node [5]. Combining scanning electron microscopy (SEM) and optical analysis along with Raman and Rayleigh scattering, we unveil the mechanism behind the light-coupling occurring at the node.

Moreover, we proved localization and field-effect control of the plasmonic resonance in semiconductor nanostructures with a spatial resolution of 20 nm. The coupling between light and collective electron density oscillations (plasmons) is exploited by nanoplasmonics to bypass the stringent limits imposed by diffraction, enabling confinement of light to subwavelength volumes. We demonstrated localization and field-effect control of the plasmon resonance in semiconductor NWs with a spatial resolution of 20 nm [6], using scattering-type scanning near-field optical microscopy in the mid-infrared region (Fig. 2). To this aim, we adopted InAs NWs embedding a graded doping profile to modulate the free carrier density along the axial direction. Our near-field measurements had a spatial resolution of 20 nm and demonstrated the presence of a local resonant feature whose position was controlled by a back-gate bias voltage. In our implementation, the field-effect induces a modulation of the free carrier density profile yielding a spatial shift of the plasmon resonance of the order of 100 nm. The relevance of our electrically tunable nanoplasmonic architectures was discussed in view of innovative optoelectronic devices concepts.

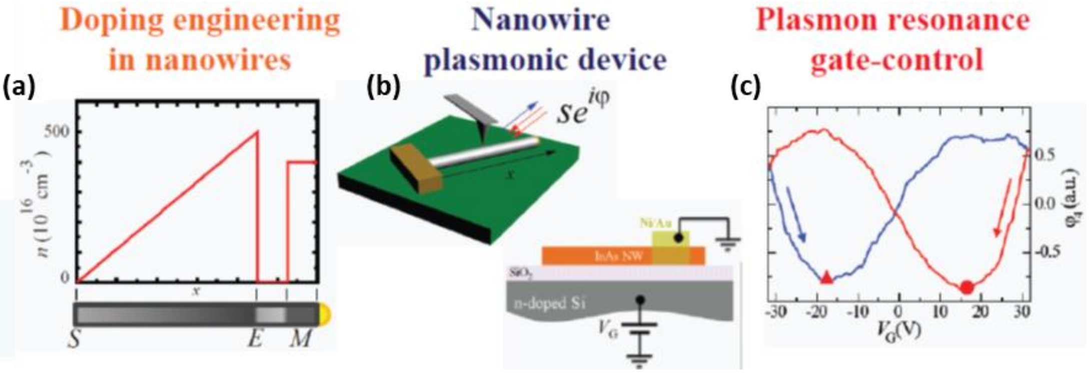

**Figure 2. (a)** We created a linear modulation of the carrier density profile *n(x)* as a function of the axial position *x* along an InAs nanowire. The induced density ranges from a nominally undoped value $n \approx 1 \times 10^{16}$ cm$^{-3}$ (in the position labeled by the letter S) to a maximum doping $n \approx 5 \times 10^{18}$ cm$^{-3}$ (in the position labeled by the letter E). An intermediate-doping segment was introduced in the growth sequence and used as marker (M) for the s-SNOM maps. The resulting graded-doping NW is sketched at the bottom of the diagram: the gray color modulation reflects the amount of doping in the NW body (with dark gray meaning high carrier concentration), while the yellow half sphere represents the metallic (Au) tip of the NW. **(b)** NWs were deposited on a $SiO_2$/Si substrate and contacted by a Ni/Au electrode. The bulk silicon was degenerately n-doped and thus can act as a back-gate upon application of a bias voltage, $V_G$ (cross-sectional sketch), provided that a ground reference is set for the NW. A $\lambda = 10.5$ µm laser beam (red arrows) is focused on an s-SNOM tip oscillating at 250 kHz. The laser impinging on the tip was vertically polarized with the wave vector forming an angle of 30° with the surface of the NW. **(c)** The amplitude *s* and phase $\varphi$ of the reflected beam (blue arrow) are detected using an interferometric pseudoheterodyne technique, demodulated at the fourth harmonic of the tip tapping frequency and used to reveal the local dielectric response of the NW. Phase modulation was achieved as a function of the gate voltage $V_G$. A strong hysteresis was observed by sweeping the gate voltage from low to high values (blue curve) and back (red curve).

Finally, we demonstrated that arrays of scatterers with subwavelength size and periodicity enable light manipulation and an extraordinary control of the light-matter interaction at the nanoscale. We proposed ensembles of subwavelength NWs – homogeneous as well as heterostructured - as an effective medium for light manipulation in reflection geometry [7,8]. We demonstrated that random assemblies of vertically aligned InAs NWs and core–shell GaAs–AlGaAs NWs display an optical response dominated by periodic modulations of the polarization-resolved reflected light as a function of the incident angle (Fig. 3). Numerical simulations clearly link the observed oscillatory effects to the semiconductor materials and the morphological features – e.g. the core and shell thickness and the tapering - of the nanostructures. Our results suggest the use of III-V NW arrays as optical meta-mirrors with perspective for sensing applications.

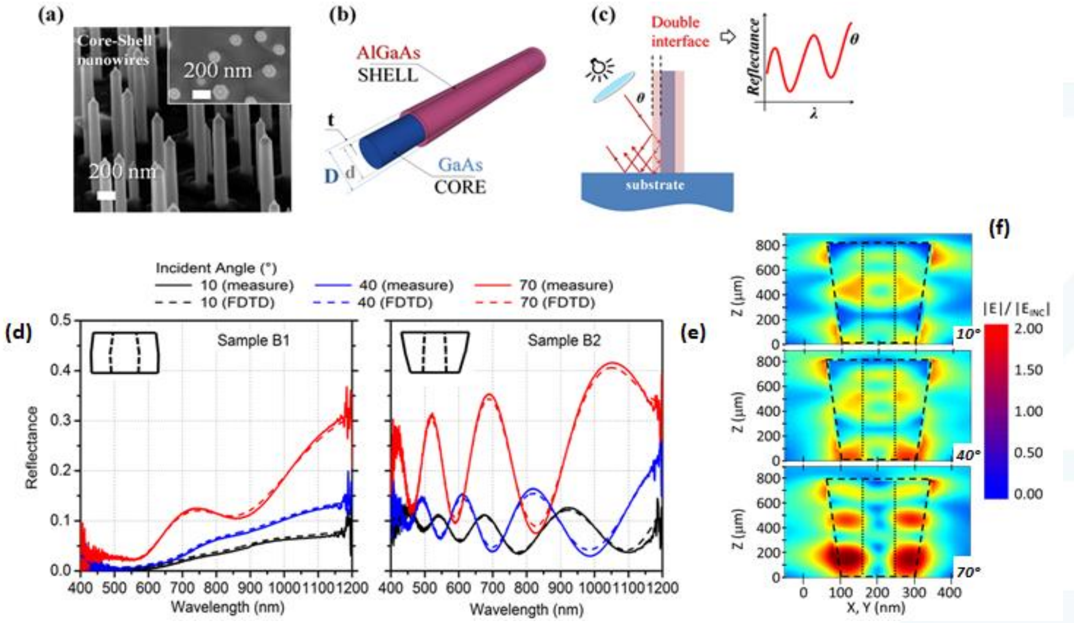

**Figure 3. (a)** 45° tilted SEM image of GaAs-AlGaAs core-shell (C-S) NWs. **(b)** Sketch of a C-S NW. **(c)** Shining light onto the lateral surface of a C-S NW. Measured (solid line) and simulated (dashed line) reflectance for a **(d)** non-tapered and **(e)** tapered C-S NW sample. **(f)** Near-field normalized electric field expansion for tapered C-S sample (incident angle is indicated).

## References

[1] S. Battiato, S. Wu, V. Zannier, A. Bertoni, G. Goldoni, A. Li, S. Xiao, X.D. Han, F. Beltram, L. Sorba, X. Xu, F. Rossella, *Polychromatic emission in a wide energy range from InP-InAs-InP multi-shell nanowires*, Nanotechnology **30**, 194004 (2019).

[2] S. Wu, K. Peng, S. Battiato, V. Zannier, A. Bertoni, G. Goldoni, X. Xie, J. Yang, S. Xiao, C. Qian, F. Song, S. Sun, J. Dang, Y. Yu, F. Beltram, L. Sorba, A. Li, B. Li, F. Rossella, X. Xu, *Anisotropies of the g-factor tensor and diamagnetic coefficient in crystal-phase quantum dots in InP nanowires*, Nano Research **12**, 2842 (2019).

[3] F. Rossella, V. Piazza, M. Rocci, D. Ercolani, L. Sorba, F. Beltram, S. Roddaro, *GHz Electroluminescence Modulation in Nanoscale Subwavelength Emitters*, Nano Lett. **16**, 5521 (2016).

[4] J. David, F. Rossella, M. Rocci, D. Ercolani, L. Sorba, F. Beltram, M. Gemmi, S. Roddaro, *Crystal Phases in Hybrid Metal–Semiconductor Nanowire Devices*, Nano Lett. **17**, 2336 (2017).

[5] F. Rossella, V. Bellani, M. Tommasini, U. Gianazza, E. Comini, C. Soldano, *3D Multi-branched SnO2 semiconductor nanostructures as optical waveguides*, Materials **12**, 3148 (2019).

[6] A. Arcangeli, F. Rossella, A. Tomadin, J. Xu, D. Ercolani, L. Sorba, F. Beltram, A. Tredicucci, M. Polini, S. Roddaro, *Gate-Tunable Spatial Modulation of Localized Plasmon Resonances*, Nano Lett. **16**, 5688 (2016).

[7] F. Floris, L. Fornasari, A. Marini, V. Bellani, F. Banfi, S. Roddaro, D. Ercolani, M. Rocci, F. Beltram, M. Cecchini, L. Sorba, F. Rossella, *Self-Assembled InAs Nanowires as Optical Reflectors*, Nanomaterials **7**, 400 (2017).

[8] F. Floris, L. Fornasari, V. Bellani, A. Marini, F. Banfi, F. Marabelli, F. Beltram, D. Ercolani, S. Battiato, L. Sorba, F. Rossella, *Strong modulations of optical reflectance in tapered core-shell nanowires*, Materials **12**, 3572 (2019).